Recent Developments of Amorphous Selenium-Based X-Ray Detectors: A Review

Heyuan Huang and Shiva Abbaszadeh, *Member, IEEE*

***Abstract*—Amorphous selenium (a-Se) is a photoconductive material that has been intensively investigated from its early application in xerography to its present application in flat panel X-ray imagers. It can be deposited up to a few millimeters thick over a large area. Its high vapor pressure yields uniform coverage in novel device structures for low-cost and large-area applications. The evidence of avalanche multiplication in a-Se and application of a-Se in high-gain avalanche rushing photoconductor video-tubes goes back to the early 1980s. Over the past decade there has been increasing research interest in novel detector structures and integration of a-Se with new materials to leverage the avalanche properties. We summarize some of the shortcomings of a-Se such as low charge carrier mobility, low charge conversion efficiency, depth dependence, and high dark current at high electric fields. We then highlight recent developments in a-Se-based devices to address these shortcomings and enable picosecond timing performance and high detection efficiency.**

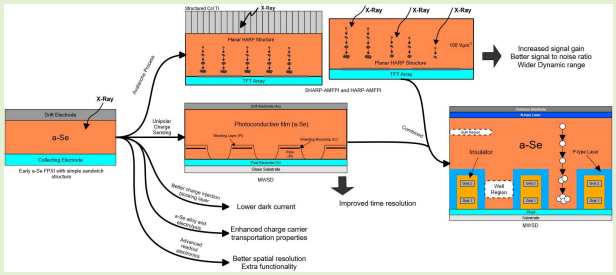

***Index Terms*—Amorphous selenium, X-ray image sensor, direct conversion, indirect conversion.**

I. Introduction

AMORPHOUS selenium has a low melting point and high vapor pressure which makes it less complex and more economical to deposit thick and uniform layers over a large area by for example thermal evaporation. Besides this advantage, amorphous selenium (a-Se) has good X-ray photoconductivity, discovered in the 1940s, and therefore can be used in X-ray imaging. a-Se was heavily used in the photocopy industry until it was replaced by inexpensive organic photoconductors in the late 1980s [1]. However, the combination of a-Se and thin film transistor (TFT) based active matrix arrays (AMA) brought a-Se back into the focus of the X-ray imaging industry. In fact, a-Se-based flat panel X-ray imagers (FPXI) have been studied extensively since the late 1990s [2]–[8].

There are several advantages of using a-Se for X-ray imaging. First, with a strong electric field applied (10 V/μm or higher) [9], a-Se exhibits excellent X-ray photoconductivity, especially in the energy range used for mammography. Second, a-Se can be deposited uniformly over a large area up to 1000 μm thick. Third, unlike many other amorphous materials, charge transport in a-Se is non-dispersive over the time scale of interest at room temperature, which allows engineers and researchers to model and predict charge behavior in a-Se-based devices relatively more easily [1]. In fact, cascade linear systems have been developed to evaluate the performance of a-Se detectors [10]–[16] and recently non-stationary models for oblique X-ray have been proposed as well [17], [18]. Additionally, because of its high resistivity, a-Se intrinsically has low dark current ($<$10 pA/mm^2 under an electric field of 10V/μm) and thermal noise compared with other candidates [19], [20]. With high bias voltage (typically higher than 70 to 80 V/μm), a-Se can also undergo an avalanche process, which dramatically increases conversion gain [1], [21], [22]. Last, but not least, a-Se direct detectors have been proven to have superior spatial resolution [23].

These advantages have kept researchers working to develop better a-Se-based X-ray imagers. With advances in electronics, the discovery of new materials, and the refinement of manufacturing techniques, many detectors with superior properties have been developed.

Manuscript received September 7, 2019; revised October 26, 2019; accepted October 26, 2019. Date of publication October 29, 2019; date of current version January 24, 2020. The associate editor coordinating the review of this article and approving it for publication was Dr. Richard T. Kouzes. *(Corresponding author: Shiva Abbaszadeh.)*

H. Huang is with the Department of Nuclear, Plasma, and Radiological Engineering, University of Illinois at Urbana–Champaign, Champaign, IL 61820 USA.

S. Abbaszadeh is with the Department of Electrical and Computer Engineering, University of California at Santa Cruz, Santa Cruz, CA 95064 USA (e-mail: sabbasza@ucsc.edu).

Digital Object Identifier 10.1109/JSEN.2019.2950319

II. Challenges of Amorphous Selenium-Based X-Ray Detectors

Although a-Se has many advantages when used in X-ray imagers, it possesses intrinsic shortcomings as well.

To improve a-Se-based X-ray detectors, we must understand the limitations of a-Se.

A. Low Charge Carrier Mobility

One of the most undesirable properties of a-Se is low charge carrier mobility. The hole drift mobility is around 0.13-0.14 cm^2/V.s, and the electron mobility is around 5-7 $\times$ 10^{-3} cm^2/V.s, which are orders of magnitude smaller than those of other common semiconductor materials like silicon (480 cm^2/V.s and 1400 cm^2/V.s for holes and electrons respectively) [1], [24]. Traditional a-Se X-ray design has a sandwich structure: two electrodes with an a-Se layer in between. Conventionally, both electrodes will be collecting charges. This implies that the complete charge collection requires the lifetime for both carriers to exceed the transit-time across the entire material thickness. But for a-Se, only the primary charge carriers (holes), the one with the greater mobility-lifetime product, can meet this condition. Additionally, because the photon interaction depth can vary across the bulk layer of a-Se, the slow signal-rise time of slower carriers can cause ballistic deficit and depth-dependent variations. All these effects eventually lead to low time resolution and high depth-dependent noise [21]. In practice, these limitations can hinder the complete charge collection of X-ray interactions, especially for breast imaging applications where a-Se is used widely because of its excellent spatial resolution [24].

B. Low Charge Conversion Efficiency

As reported by previous studies [24], [25], the charge conversion efficiency of a-Se is not ideal, mostly because of its high ionization energy. The electron-hole pair creation energy of a-Se at an applied field of 10 V/μm is 45-50 eV [26], [27], while other semiconductor materials, such as HgI_2 and silicon, have electron-hole pair creation energy equal to or less than 5 eV under the same electric field [28]. Additionally, the charge conversion of a-Se is highly dependent on the applied field [29]–[31], and therefore an a-Se-based detector is typically operated at 10 V/μm or higher to generate desirable readout. But the high applied field will inevitably cause charge injections and therefore increase dark current. If not addressed properly, the low charge conversion of a-Se will result in a small signal to noise ratio and hence low energy resolution.

C. Depth Dependence

There are two instances where the depth dependence can have influence: the charge collection process and the avalanche process (if the detector involves an avalanche process). During the charge collection process, both the charge collection efficiency and the time needed for maximum collection are dependent on the thickness of the detector or the interaction depth. Previous studies regarding the X-ray sensitivity of a-Se, which is defined as the charge collected per unit area per unit exposure of radiation, have suggested a dependence of X-ray sensitivity on the thickness of detectors [32], [33]. Another study provided simulated results of a 200-μm a-Se traditional planar parallel-plate detector with an applied field of 13 V/μm [21] to demonstrate the time dependence. The results showed that a shorter distance between interaction and the collecting electrode (negative electrode for a-Se detectors) will lead to less time needed for complete charge collection: with the thickness of the detector being L, when the interaction is $0.9L$ away from the collecting electrode, the complete charge collection time is 1.2 μs, and the time reduces to about 0.7 μs if the distance is $0.5L$ and approximately 0.2 μs at $0.1L$.

In the avalanche process, the farther the initial charge travels, the more energy it will accumulate and the more secondary charges will be created. Therefore, it is possible that interactions with the same amount of energy but at different depths will produce different energy readouts. The depth dependence can hence undermine both time and energy resolution. A previous study has shown that a huge avalanche gain fluctuation existed when X-rays are absorbed over a thick layer [25]. Generally, the multiplication factor M depends exponentially on the thickness of the photoconductor layer [34], [35]. This suggests that the avalanche layer should be both thin and separated from the absorption layer.

D. Dark Current

Intrinsically, a-Se has a relatively small dark current at room temperature compared to competing photoconductors. In X-ray imaging, however, a-Se is in contact with two metal electrodes with a strong bias electric field applied in order to achieve sufficient X-ray photogeneration efficiency. The strong field will inevitably increase the dark current inside a-Se by hole injections from the positive electrode, which is especially evident for direct conversion detectors [36]. The resulting high dark current will reduce the dynamic range of the device [37]. In medical imaging applications, the dark current of a-Se should be reduced to less than 10 pA/mm^2 [38].

III. Development and Emerging Technologies

Recent studies have focused on the development of better a-Se X-ray detectors by taking advantage of the intrinsic properties of a-Se, designing novel detector structures and combining a-Se with other materials and better pixel sensors to overcome the downside of a-Se and provide better detector performance.

A. The Use of the Avalanche Process

One advantage of a-Se is its ability to undergo an avalanche process if a strong electric field is applied (normally higher than 70 V/μm [25] to 80 V/μm) [1], [21]. Above the voltage threshold the effective quantum efficiency can increase several orders of magnitude, while the multiplication factor depends on the thickness of a-Se layer. According to the data from previous studies [1], [39], four a-Se devices with thicknesses of 35 μm, 25 μm, 15 μm and 8 μm have all shown a significant increase in effective quantum efficiency once the bias voltage passed 80 V/μm. At 100 V/μm, the effective quantum efficiency reached about 1000 for a 35 μm thick a-Se layer, 300 for 25 μm, 200 for 15 μm, and 100 for 8 μm. A separate study also achieved maximum gain of 1000 for a 35 μm thick

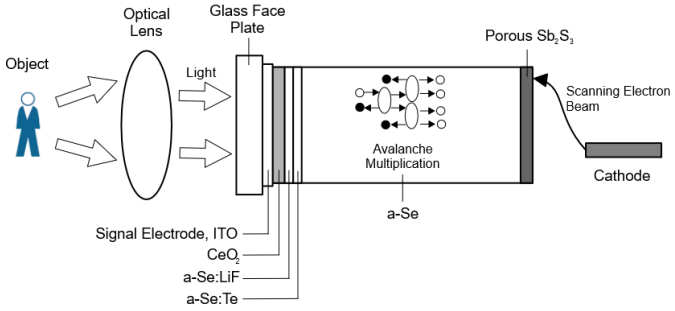

Fig. 1. HARP video tube with avalanche gain (adapted from [1]).

a-Se layer with a field of 92 V/μm [40]. The avalanche process occurs when the holes (primary charge carriers) inside the a-Se gain energy faster than losing it to phonons and hence produce impact ionization [34], [41]. There are two important features of the avalanche process inside a-Se: firstly, the slow charge carriers inside a-Se, i.e. electrons, are not involved in this process [1], [40], [42]–[45]; secondly, the avalanche process is non-Markovian and, with a design that suppresses depth-dependent gain, the additional noise from the avalanche has limited impact on the signal to noise ratio [42], [46], [47].

The avalanche process improves the low charge collection efficiency of a-Se. One early application of the avalanche process inside a-Se was the High-gain Avalanche Rushing Photoconductor (HARP) camera [48]–[50]. The original HARP detector (shown in Fig. 1) worked with visible light and was used for commercial TV pickup tubes. It was deposited on a glass substrate with indium tin oxide (ITO) as a transparent anode, facing the incoming signal and biased positively. The entire target is around 25-35 μm thick. CeO_2 and a-Se doped with LiF (a-Se:LiF) are placed between a-Se and the anode to serve as hole injection blocking layer. There is also an additional layer of a-Se doped with Te (a-Se:Te) as photo-generation layer. Readout consists of a cathode with scanning electron bean and a porous Sb_2S_3 layer as an electron injection blocker.

The HARP concept is still widely used by many types of X-ray imagers. With developments in readout electronics and crystal manufacturing, new HARP modalities have been created. One type of detector has a scintillator layer between the X-ray source and the a-Se layer so that the a-Se layer with avalanche process serves a similar purpose as conventional photomultiplier tubes and silicon photomultipliers. This type of indirect conversion imager is referred to as Scintillator HARP Active Matrix Flat Panel Imager (SHARP-AMFPI), as shown in Fig.2(a). The other type of HARP detector shares similar designs, except that the scintillator layer is not included, and the detector therefore employs direct conversion, which means that the X-ray photon generates electron-hole pairs inside a-Se directly. This type is called HARP-AMFPI [51], as shown in Fig.2(b).

Indirect conversion has been suggested to be more suitable for avalanche X-ray imagers [52], [53]. Visible photons emitted by scintillators are mostly absorbed by a-Se at the surface of the photoconductor, while diagnostic X-rays require an a-Se thickness of 200-1000 μm to reach sufficient quantum efficiency. Therefore, not only will the applied voltage have to be significantly high in order to achieve avalanche field, but also avalanche gain fluctuation due to depth dependence will be problematic. SHARP-AMPFI performs well for different medical imaging applications, such as breast imaging and radiography-fluoroscopy. Nonetheless, because of the omni-directional propagation of light, indirect conversion detectors have inferior resolution in terms of the modulation transfer function (MTF) compared to direct conversion detectors. The MTF is the Fourier transform of the point spread function and is a measure of how the system translates details of the objects being imaged to the images themselves.

On the other hand, direct conversion X-ray imagers, including HARP-AMPFI, not only provide better MTF, but also have large dynamic range and reduction of the electronic noise produced by very high gain. However, the photon-to-charge conversion and carrier mobility issue are very evident for direct conversion detectors and thus this detector is limited by low X-ray quantum efficiency and depth-dependent avalanche gain (g_{av}), which also reduces the Swank factor [54]. To mitigate the unwanted depth dependence, the thickness of a-Se is supposed to be larger than is required for X-ray absorption. Therefore, HARP-AMPFI is best suited for very low energy X-rays, such as 6-8 keV for protein crystallography [55].

To summarize, incorporating a-Se HARP structures is the proper direction of development for both direct conversion detectors for low energy applications and indirect conversion detectors for fluoroscopic applications [27], [35], [56].

Several studies have investigated the use of the avalanche process of a-Se in medical imaging applications [47], [54], [56]–[60] as well as crystallography [55], [61]. Yet these studies did not fully extend to large area FPXI. A later study assessed the feasibility of large area FPXI with avalanche gain and concluded such a structure could achieve fully quantum noise limited X-ray imaging with high resolution [53]. The feasibility of depositing HARP structure on a TFT array was practically demonstrated in 2015 [62], [63]. A year later, Scheuermann and coworkers have successfully deposited the HARP structure onto a TFT panel with an area of 24×30 cm^2 and pixel pitch of 85 μm [51]. Under an electric field of 105 V/μm, the detector achieved an avalanche gain of 15 ± 3 for direct conversion and 76 ± 5 for indirect conversion. The study also demonstrated that with high g_{av}, the effect of electronic noise can be substantially reduced because of the increased signal to noise ratio provided by the increased quantum detection efficiency. The group proposed that improving the optical coupling efficiency between the scintillator and HARP can reduce the required avalanche gain for quantum noise limited detector operation at low dose.

In 2017, the first prototype SHARP-AMPFI was fabricated by Scheuermann's team [64]. The prototype was deposited on a 24×30 cm^2 TFT array with a pixel pitch of 85 μm and consisted of a 16-μm a-Se layer and a 105-μm CsI:Tl scintillator layer. The applied field reached 105 V/μm without breaking down the a-Se and an avalanche gain of 76 ± 5 was measured under that field, which was demonstrated to be able to amplify the signal enough to overcome the electronic noise.

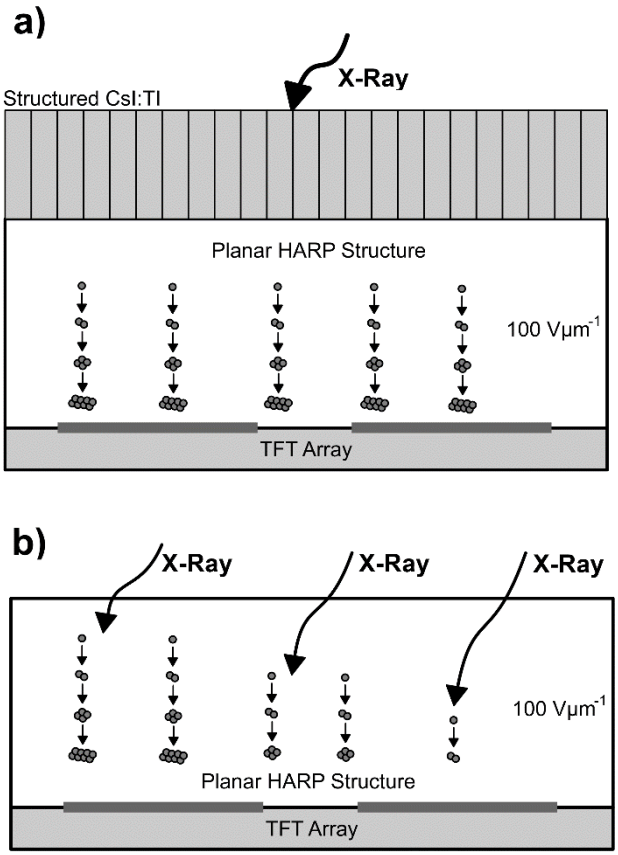

Fig. 2. (a) SHARP-AMFPI and (b) HARP-AMFPI design (adapted from [26]).

Yet, this system has poor optical transparency of the high-voltage electrode and long integrating time which leads to dark current noise. The combined effect was the dominance of high-spatial frequency noise in imaging performance.

B. The Manipulation of Electric Field

The electric field inside a-Se materials plays a decisive role in the charge carrier transport and collection. A properly shaped electric field inside the a-Se can mitigate the poor charge transport issue and therefore improve time resolution.

Weighting potential is an important concept describing the relationship between the charge collection and instantaneous position of carriers. As provided by Shockley [65] and Ramo [66], the induced charge $Q(t)$ due to the motion of a single electron can be calculated as:

$$Q(t) = qV_W(z) = qV_W(\mu Ft) \tag{1}$$

where q is the charge of an electron, $V_W(z)$ is the weighting potential in the bulk, z is the carrier displacement, μ is the effective drift/hopping mobility, F is the applied electric field, and hence within time t, $z = \mu Ft$.

The induced current can be expressed as:

$$i(t) = q\vec{v} \cdot \vec{F}_W = q\frac{\partial V_W}{\partial t} = q\mu F\frac{\partial V_W}{\partial z} \tag{2}$$

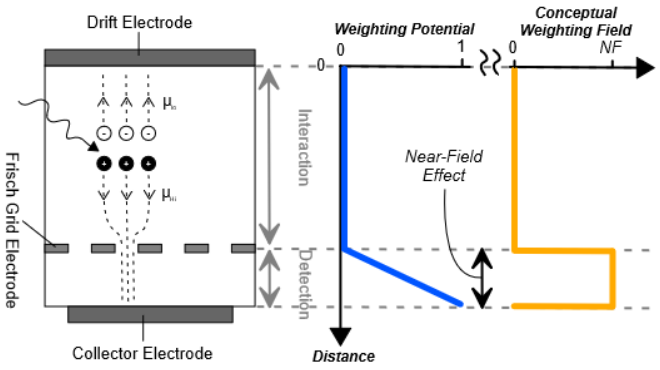

Fig. 3. The electric field and weighting potential that created the near-field effect (adapted from [21]).

where $\vec{v}$ is the instantaneous velocity and $\vec{F}_W$ is the conceptual weighting field vector. Equations (1) and (2) indicate that the detected signal is related to the weighting potential.

Unipolar charge sensing is another crucial principle where the detector preferentially senses the charge carriers with a higher mobility-lifetime product while remaining insensitive towards the movement, trapping, and release of slower carriers [21]. This preferential sensing can be realized by the weighting potential which has a strong increasing gradient only in the region near the collecting electrode while increases very gradually elsewhere [67]. Achieving such weighting potential is possible with near-field effect or small pixel effect [68]. The near-field/small-pixel effect occurs when the pixel pitch is equal to or less than one tenth of the thickness of the detector [69], and such small pixel will sense the movement of carriers only when they are very close to the pixel. However, in some a-Se devices the near-field effect is not practically achievable because the thickness of the a-Se layer is relatively small (e.g., 200 μm for mammography panels) compared to the pixel pitch (e.g., 85 μm in regular mammography panels) [64]. Nonetheless, the equation (1) suggests that the instantaneous weighting potential sensed by the carrier is dependent on the instantaneous position of that carrier, and because the position is determined by the applied field and time, the near-field effect inside a-Se detector can still be created by manipulating the electric field.

Goldan and Karim proposed to insert a Frisch grid (or mesh) electrode in front of the collecting (pixel) electrode to shape the electric field inside the a-Se [67], as shown in Fig.3. The simulation results demonstrated that the desired weighting potential for the near-field effect (i.e. raising rapidly only near the collection electrode) can be created by a Frisch grid. This was confirmed by later studies [70], [71]. Recently, this design has been further improved and prototyped [21]. In addition, they have successfully implemented unipolar time differential (UTD) charge sensing, where the impulse function is proportional to the time derivative of that in a conventional planar detector design. With UTD charge sensing, the transit-time of secondary charges will no longer limit the signal rise time for 100% charge collection efficiency. Therefore, the UTD can enable the detector to approach the theoretical limit of time resolution. The team has successfully achieved

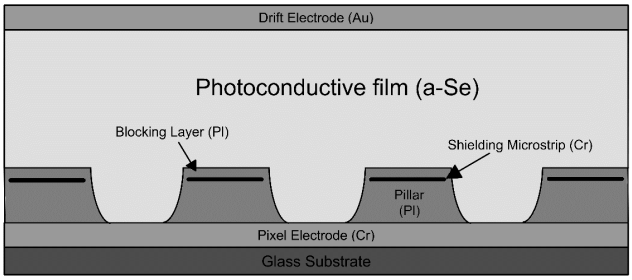

Fig. 4. The schematic diagram of the prototyped MWSD (adapted from [21]).

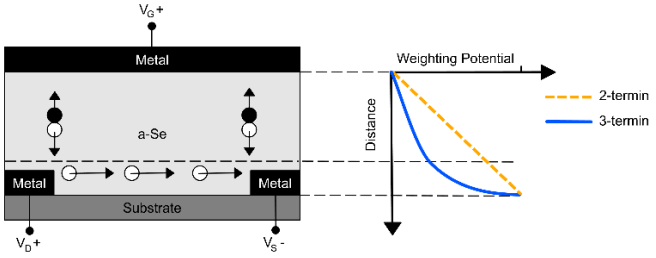

Fig. 5. The structure of the three-terminal design and the achieved weighting potential.

ultra-fast signal rise time which is limited only by the size of the primary charge carrier (hole) cloud. The prototyped device is referred as the Multi-Well Solid-state Detector (MWSD), shown in Fig.4. The MWSD has been tested and shown a reduction in signal rise time by a factor of ∼300, compared with conventional planar parallel-plate detectors.

Another detector concept achieving unipolar charge sensing is the three-terminal design [72]. As the name suggests, this design differs from conventional structure by having three terminals instead of two, which are denoted as gate G (VG), source S (VS) and drain (VD). The structure is demonstrated in Fig.5.

The three-terminal design also seeks to enhance the electric field near the collecting electrode, but unlike the MWSD (where the boosted electric field is still in the vertical direction), the three-terminal detector increases the field in the lateral direction with terminals S and D. The G terminal is used to shape the electric field so that an evenly increasing vertical field still exists in order to facilitate the drifting of induced charges. Therefore, the detector is virtually divided into two layers: the top charge generation layer with a gradually increasing vertical electric field and the bottom charge collection layer with a very strong lateral field. The simulation analysis showed a weighting potential fits the profile needed for unipolar charge sensing. Although the weighting potential was not as perfect as the one achieved by MWSD, the simulation was still able to demonstrate the unipolar charge sensing capability of this design. An additional advantage of the three-terminal design is that the G terminal can control the current between the S and D terminals, and therefore the transfer and output characteristics of the detector can be readily controlled. This advantage can potentially help avoid using a TFT switch at the pixel level. However, this design is yet to be fabricated or prototyped.

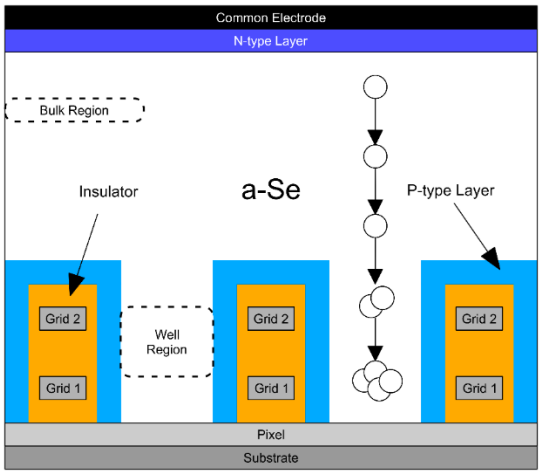

Fig. 6. The schematic diagram of the SWAD multi-grid structure (adapted from [25]).

Goldan and coworkers later combined the concept of MWSD with HARP and proposed another design called field-Shaping multi-Well Avalanche Detector (SWAD), shown in Fig.6. It implements an avalanche zone inside the well region by introducing an additional Frisch grid layer. Hence, the two separate regions within SWAD become: (1) bulk region (up to 1 mm thick for X-ray absorption) with relatively weak field (∼10 V/μm) where the X-ray interaction happens and produces electron-hole pairs, (2) avalanche region with strong field (∼80 V/μm) inside wells where the primary charge carriers (holes) get multiplied [25].

When the detector is exposed to an X-ray source, the incoming radiation will be absorbed in the bulk region, producing electron-hole pairs. Then the primary charge carriers (holes), will drift into the well regions where they undergo the avalanche process. The multiplied signal will eventually be collected by the collector electrode. The two Frisch grids provide more precise control of the field inside the detector. By properly biasing the grids, field lines inside well regions can terminate on the collecting electrode instead of well walls, which resolves the high dark current issue found in previous MWSD design because of charge injection [73].

Currently, the SWAD has not been manufactured. However, two successive studies [24], [25] have used simulations to evaluate the performance of the SWAD and revealed its potential of becoming a photon-counting detector. The energy resolution of the SWAD is expected to be comparable to current CdTe detectors [25], [74]. Another recent simulation study also concluded that the SWAD is capable of attaining the necessary count rate linearity to achieve photon counting performance while obtaining energy resolution which is comparable to that of the CdTe based detectors for a 1 mm^2 pixel [75].

Another recently prototyped design combining UTD and HARP with the insertion of Frisch grid was fabricated using nanoscale structures [42]. The detector has a high-density multiwell geometry with nanoscale pillars and one layer of nano-Frisch grid. The experiment was carried out with a picosecond laser, and the results showed that the detector improved the temporal performance of a-Se by nearly 4 orders of magnitude,

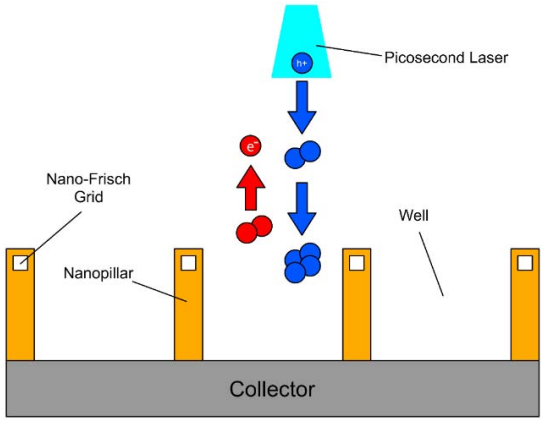

Fig. 7. The schematic diagram of the picosecond multiwell selenium detector experiment (adapted from [42]).

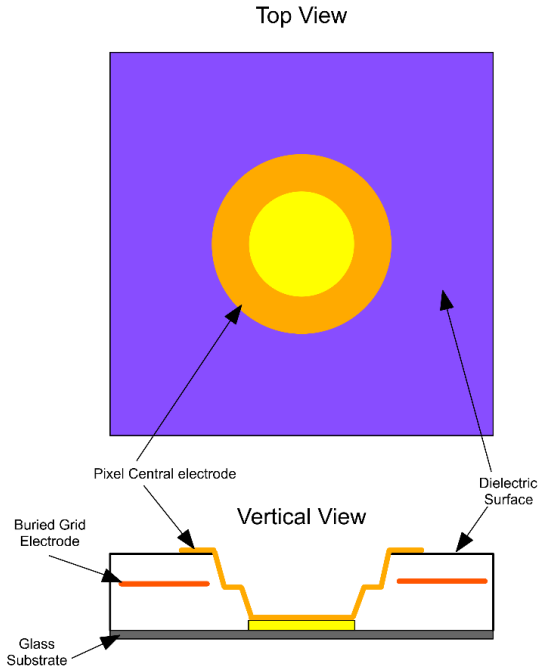

Fig. 8. The schematic diagram MPPC detectors (adapted from [76]).

allowing the detector to reach picosecond resolution. The experiment and detector design are shown in Fig.7. This nano structure design also has the potential application in positron emission tomography (PET) scanners as a replacement of silicon optical sensors.

The improvement on the time resolution of a-Se-based X-ray detectors has shown enough potential that the application of a-Se detectors for real-time imaging has been investigated. A recent study proposed and prototyped a design called the Multi Pixel Proportional Counter (MPPC) [76], [77], shown in Fig.8. The MPPC was intended to overcome two major issues that keep a-Se from real-time imaging use [39]: 1) X-ray sensitivity needs to be further improved or the noise further reduced so that the quantum noise limit can be satisfied even at extremely low exposure, which is true for real-time imaging where essentially several images need to be taken within a second. 2) the detector should operate at a high frame rate (30fps) without suffering from memory artifacts.

Compared to static imaging, real time imaging usually involves high energy photons and thus requires a-Se to be relatively thick to achieve the desired absorption of incoming photons. For example, photons with mean energy of 60 keV require the thickness of the photoconductor to be about 1000 μm. Although a-Se has the advantage of convenient and uniform deposition as a thick film, the sensitivity will be limited by Schubweg which is defined as a carrier drift range before being deeply trapped. Plus, as mentioned before, in conventional a-Se detector structure the depth dependence can noticeably influence both time and energy resolution, and it will inevitably be worsened with a thicker layer of a-Se. Therefore, simply depositing a very thick layer of a-Se to match the requirement for high energy X-ray absorption is not practical.

Memory artifacts arise primarily from two sources: lag and ghosting. Lag is the residual signal after an x-ray exposure and ghosting is the change in x-ray sensitivity as a result of previous exposures [78]. Normally, the sensitivity reduction is insignificant if operated under proper conditions [79]. However, in real-time imaging lag will cause the subsequent frame to carry spillover from the previous exposure and therefore produce inaccurate or misleading images, especially for a thick layer of a-Se where lag is increased by poor charge transportation. As suggested by a previous study, the main source of photocurrent lag is the release of the trapped charge, i.e. electrons inside a-Se [77].

Similar to SWAD, MPPC utilizes avalanche gain and unipolar charge sensing to overcome the two problems mentioned above. Avalanche gain helps increase the signal gain while unipolar charge sensing reduces the temporal artifacts by ignoring the behavior of electrons. MPPC also utilizes a Frisch grid to help shape the electric field, along with a SiN layer to prevent charge injection. A major difference between MPPC and SWAD is that MPPC operates in two phases: accumulation and collection. The accumulation phase is where all the primary charge carriers (holes) will accumulate on the insulator layer surrounding the negatively biased Frisch grid. The insulator also prevents charge injections at the same time. During the collection phase, the grid voltage is reversed, and electric field lines will bend towards the pixel electrodes. The pixel electrodes possess a unique octagonal well structure so that the convergence of the electric field occurs near the pixel electrodes where the avalanche process will happen.

The prototyped MPPC device has shown a significantly reduced lag: only around 20% of that found in conventional a-Se devices. The device was also observed to have substantially improved temporal performance.

C. Charge Injection Blocking

The major reason for the increased dark current within a-Se under high biased voltage is charge injection, primarily the injection of holes from positive electrodes [73]. Therefore, dark current can be significantly reduced by placing an injection blocking layer between the electrodes and a-Se.

A common approach is to place n-type and/or p-type layers between the a-Se and corresponding electrodes, forming an n-i, i-p or even n-i-p multiplayer structure [1], [80]. This method can effectively reduce the dark current to an acceptable level with an applied field of 10 V/μm. However, emerging applications and design advancements of a-Se detectors normally can benefit from increased signal gain, usually achieved by the increase of bias voltage. For example, the HARP, SWAD, and MPPC detectors mentioned above all take advantage of the avalanche process inside a-Se, which requires an electric field higher than 70-80 V/μm. Considering the dark current limit of 10 pA/mm^2 for medical imaging applications, n-type and/or p-type layers may no longer provide the desired dark current reduction under such high voltage. Consequently, many studies have investigated proper charge injection blocking material. Aside from C_{60} [81], perylene tetracarboxylic bisbenzimidazole (PTCBI) [82], CeO_2 [83] and zinc oxide (ZnO) [84], more promising materials have been studied recently.

Abbaszadeh and her team investigated multiple types of material for a hole injection blocking layer for indirect X-ray conversion [82], including CeO_2, TiO_2, PTCBI and polyimide (PI). CeO_2 has been used already as a blocking layer in some high voltage detectors such as HARP, with TiO_2 sharing similar properties. Both PTCBI and PI are promising materials with very low hole mobility and industrial insulating properties respectively. It was reported that the dark current with CeO_2 and TiO_2 is high when the electric field exceeds 40 V/μm, indicating that they might not be the ultimate choice of blocking layer for detectors operating under high voltage. Additionally, these two materials are very sensitive to deposition conditions, which complicates the fabrication process. The PTCBI could have been a good candidate because of the proportionality between its thickness and reduction of dark current, but it is found to have less blocking capability than CeO_2 and TiO_2. On the other hand, PI is found to have the most desirable properties among all four tested materials. PI can maintain sufficiently low dark current (less than 10 pA/mm^2) even under voltage as high as 92 V/μm, and strong charge accumulation is not found in the detector. A later study also confirms that PI does not degrade the performance of a-Se. Instead, it helps to improve the lag issue, despite the trade-off between ghosting and dark current [85]. Moreover, PI is subsequently found to be suitable as a buffer between a CMOS panel and a-Se, which inhibits the problem of crystallization and improves the stability of the detector [86]. The PI layer between CMOS and a-Se has successfully been showed to push the limit of MTF toward the material limit.

As mentioned before, a-Se can also be used as an indirect conversion X-ray detector or as an optical detector. In these applications, the thickness of the a-Se layer can be less than 1 μm. As a consequence, the voltage drop across PI, an insulator hole blocking layer, will not be trivial. Therefore, it is better to use metal oxide as the hole blocking layer under these circumstances [87]. Abbaszadeh and her team showed that Indium Gallium Zinc Oxide (IGZO) is an appealing choice [88]. The IGZO provides an exceptional reduction of dark current. Even with 60 V/μm of biased voltage, a 375-nm IGZO layer still managed to maintain a dark current under 1 pA/mm^2.

Another group showed that aluminum oxide and hafnium oxide (ALD-HfO_2) is a good candidate as well [89]. At 15 V/μm, the addition of an ALD-HfO_2 blocking layer inside the metal-insulator-semiconductor-insulator-metal photodetector improved the optimal signal contrast to more than 500 times the contrast of a photodetector without any blocking layer.

D. Impurities

Normally, commercial selenium is well-purified, primarily because impurities can create point defects, acting as points for charge trapping and recombination. They can also cause charge build-up, influence electric field and limit the detector performance. However, the addition of certain impurities can also help stabilize a-Se and improve both physical and electric properties. For instance, Arsenic (As) can be added to prevent crystallization [36], [38], and Chlorine (Cl) can improve charge transport properties [90]. Studies have reported that the presence of Cl inside a-Se will compensate for hole traps and enhance electron trapping and therefore increase the lifetime of holes while decreasing electron lifetime [91], [92]. The basic mechanism of Cl in a-Se is that Cl involves a series of two reactions that transform under-coordinated charge defects Se_1^- into over-coordinated ones Se_3^+ [91].

$$Se_1^- + Cl_1^0 \rightarrow Se_2^0 + Cl_0^-$$
$$Se_2^0 + Cl_1^0 \rightarrow Se_3^+ + Cl_0^-$$

The most straightforward way of introducing an impurity into a-Se is through synthesis of Selenium alloys or doping [93]–[95]. Recently, Chowdhury's group has synthesized a high resistivity a-Se (As, Cl) alloy through a custom deposition setup [96]. Tests have shown that the synthesized a-Se alloy (As 0.52%, Cl 5ppm) has resistivity of $2 \times 10^{14} \Omega \cdot cm$, which is suitable for high resolution radiation detection and dark current of only a few pA/mm^2, which fulfills the requirement for medical imaging use. The bulk properties and physical properties, including melting point and crystallization temperature, were also reported to be improved.

Another way of introducing Cl impurities is through electrolysis [97], [98]. During the electrolysis process, a-Se is used as the anode to electrolyze a saturated NaCl solution. Through the attraction of the positive anode, the anion Cl- will be introduced into the a-Se. A previous study has shown that Cl can submerge for more than 60% of the a-Se film thickness [97]. The process is demonstrated in Fig.9.

Another study has investigated the combination of heterostructure and electrolysis to "design" the transportation properties of multilayer a-Se films [90]. The heterostructure is typically used in high performance photoelectronics because of its energy gap variations allowing the control of charge carrier flow [99]. One example of heterostructure usage for a-Se is the HARP detector [87], [100]. After electrolysis, the device showed higher conduction current and better photoresponse.

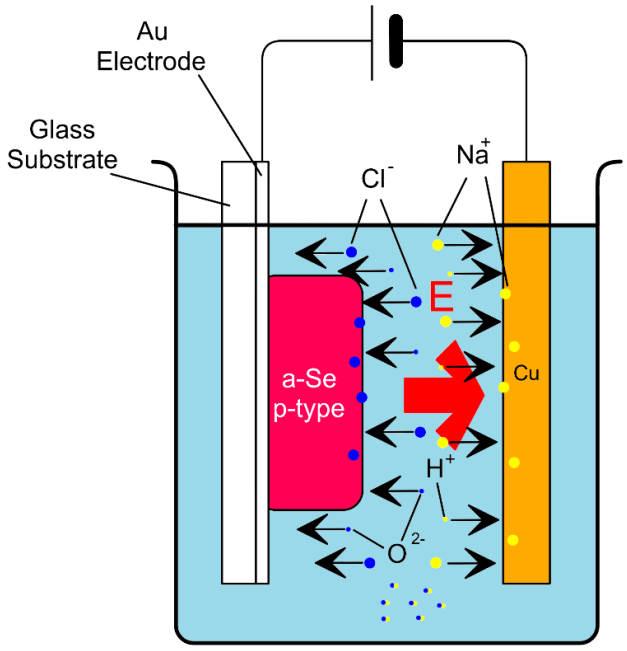

Fig. 9. Illustration of typical a-Se electrolysis (adapted from [97]).

One advantage of electrolysis is that it can be used on a-Se films that have already been deposited. Therefore, it can be a very flexible and effective way of modifying the property of a-Se panels.

E. Combination With Advanced Pixel Sensors

As the final component to convert charges into digital signals, pixel sensors are the key to ensure that the improvement of the performance of a-Se translates properly into better image quality. In fact, as mentioned before, the comeback of a-Se into the X-ray imaging industry can be attributed to the application of a-Si:H TFT based AMA in the medical imaging industry to manufacture FPXIs. Since the first a-Se-based FPXI was prototyped in the mid-nighties [101]–[107], the digital sensor industry has made significant progress, including the invention and improvement of CMOS imager sensors. For a-Se FPXIs, both a-Si:H TFT-AMA and CMOS based detectors are of interests. While CMOS can offer additional functionalities and faster speed, a-Si:H TFT-AMA is better for large area applications and costs less [27]. Additionally, although both sensors have tradeoffs between spatial resolution and image noise, each of them is suited better for different scenarios [108]: the a-Si:H flat panel detectors have slightly better performance for low-contrast visualization, i.e. emphasizing low-frequency response, while the CMOS flat panel detectors perform better for high-contrast visualization or emphasizing high-frequency response.

Because a-Se intrinsically has good spatial resolution, combining a-Se with high-resolution pixel sensors is one direct way to improve the spatial resolution of the detector as a whole. Several studies have investigated the integration of a-Se with high-resolution CMOS panels. Scott et al have successfully manufactured an a-Se-based direct conversion CMOS X-ray detector with pixel pitch of 25 μm [86]. The fabricated device was shown to approach the fundamental material limit of MTF, i.e. the MTF is limited only by a-Se properties instead of the pixel sensors. Later, Scott, Parsafar et al fabricated a high-dose CMOS a-Se direct conversion X-ray detector with 5.6 μm $\times$ 6.25 μm pixel pitch and a much higher gain in DQE compared with existing scintillator-based imagers [109], [110]. Another recent study by Camlica et al has reported a prototype direct conversion X-ray detector with 11 μm $\times$ 11 μm pixel pitch and single-photon-counting ability [111]. The prototype detector combined a-Se with CMOS and overcame the count-rate limit of a-Se by unipolar charge sensing, which is achieved by the unique pixel geometry enabling the small pixel effect.

As for TFT sensors, studies have been focused on developing better pixel structure to improve their performance and functionality. An intelligent pixel architecture was developed by Karim et al in 2007, which enabled on-pixel amplification and therefore reduced the effect of external readout noise [112]. Later Wang and coworkers successfully prototyped a large-area indirect conversion detector based on a-Se and a-Si:H TFT [113]. The fabricated 32 $\times$ 32 micro-pixel detector was reported to have very fast integration and showed great promise for low light detection. Another team from Taiwan created a mechanically flexible direct conversion X-ray detector consisting of a micropillar structured a-Se layer and a flexible TFT backplane [114]. The detector was suggested to be bendable, i.e. it was able to capture an X-ray image when it was curved.

IV. Conclusion

Recent developments of a-Se X-ray detectors focus on alleviating its intrinsic limitations. Taking advantage of the avalanche properties amplifies the signal and increases the signal to noise ratio. Shaping the electric field properly allows only the primary charge carriers to be sensed and improves the time resolution. Using the right blocking materials reduces charge injection and mitigates the dark current problem. Introducing impurities modifies the physical and electrical properties of a-Se and makes it more suitable for imaging applications. Combining a-Se with better pixel sensors achieves higher resolution and additional functionality. Prototyped novel detectors have shown excellent time response and detection efficiency along with the intrinsic high spatial resolution of a-Se. Future works could combine these existing concepts and push the performance of a-Se X-ray detectors closer to the theoretical limit.

References

[1] S. Kasap *et al.*, "Amorphous selenium and its alloys from early xeroradiography to high resolution X-ray image detectors and ultrasensitive imaging tubes," *Phys. Status Solidi (B)*, vol. 246, no. 8, pp. 1794–1805, 2009, doi: 10.1002/pssb.200982007.

[2] G. Pang, W. Zhao, and J. A. Rowlands, "Digital radiology using active matrix readout of amorphous selenium: Geometrical and effective fill factors," *Med. Phys.*, vol. 25, no. 9, pp. 1636–1646, 1998, doi: 10.1118/1.598344.

[3] N. Matsuura, W. Zhao, Z. Huang, and J. A. Rowlands, "Digital radiology using active matrix readout: Amplified pixel detector array for fluoroscopy," *Med. Phys.*, vol. 26, no. 5, pp. 672–681, 1999, doi: 10.1118/1.598572.

[4] G. Pang, D. L. Lee, and J. A. Rowlands, "Investigation of a direct conversion flat panel imager for portal imaging," *Med. Phys.*, vol. 28, no. 10, pp. 2121–2128, 2001, doi: 10.1118/1.1405844.

[5] G. Pang and J. A. Rowlands, "Development of high quantum efficiency flat panel detectors for portal imaging: Intrinsic spatial resolution," *Med. Phys.*, vol. 29, no. 10, pp. 2274–2285, 2002, doi: 10.1118/1.1507779.

[6] W. Zhao, W. G. Ji, A. Debrie, and J. A. Rowlands, "Imaging performance of amorphous selenium based flat-panel detectors for digital mammography: Characterization of a small area prototype detector," *Med. Phys.*, vol. 30, no. 2, pp. 254–263, 2003, doi: 10.1118/1.1538233.

[7] D. C. Hunt, O. Tousignant, and J. A. Rowlands, "Evaluation of the imaging properties of an amorphous selenium-based flat panel detector for digital fluoroscopy," *Med. Phys.*, vol. 31, no. 5, pp. 1166–1175, 2004, doi: 10.1118/1.1707755.

[8] W. Zhao, D. C. Hunt, K. Tanioka, and J. A. Rowlands, "Amorphous selenium flat panel detectors for medical applications," *Nucl. Instrum. Methods Phys. Res. A, Accel. Spectrom. Detect. Assoc. Equip.*, vol. 549, nos. 1–3, pp. 205–209, 2005, doi: 10.1016/j.nima.2005.04.053.

[9] N. Hijazi, D. Panneerselvam, and M. Z. Kabir, "Electron–hole pair creation energy in amorphous selenium for high energy photon excitation," *J. Mater. Sci., Mater. Electron.*, vol. 29, no. 1, pp. 486–490, 2018, doi: 10.1007/s10854-017-7937-8.

[10] W. Zhao, W. G. Ji, and J. A. Rowlands, "Effects of characteristic X rays on the noise power spectra and detective quantum efficiency of photoconductive X-ray detectors," *Med. Phys.*, vol. 28, no. 10, pp. 2039–2049, 2001, doi: 10.1118/1.1405845.

[11] S. M. Arnab and M. Z. Kabir, "Impact of charge carrier trapping on amorphous selenium direct conversion avalanche X-ray detectors," *J. Appl. Phys.*, vol. 122, no. 13, 2017, Art. no. 134502, doi: 10.1063/1.5000510.

[12] M. Rabbani, R. Shaw, and R. Van Metter, "Detective quantum efficiency of imaging systems with amplifying and scattering mechanisms," *J. Opt. Soc. Amer. A*, vol. 4, no. 5, pp. 895–901, 1987, doi: 10.1364/josaa.4.000895.

[13] A. Cunningham, *Handbook of Medical Imaging*, vol. 1, J. Beutel, H. L. Kundel, and R. L. van Metter, Eds. Washington, DC, USA: SPIE, 2000.

[14] J. G. Mainprize, D. C. Hunt, and M. J. Yaffe, "Direct conversion detectors: The effect of incomplete charge collection on detective quantum efficiency," *Med. Phys.*, vol. 29, no. 6, pp. 976–990, 2002, doi: 10.1118/1.1477235.

[15] M. Z. Kabir and S. O. Kasap, "DQE of photoconductive X-ray image detectors: Application to a-Se," *J. Phys. D, Appl. Phys.*, vol. 35, no. 21, pp. 2735–2743, 2002, doi: 10.1088/0022-3727/35/21/308.

[16] J. Tanguay, N. Mantella, J. Stavro, I. A. Cunningham, A. H. Goldan, and W. Zhao, "Cascaded-systems analysis of signal and noise in contrast-enhanced spectral mammography using amorphous selenium photon-counting field-shaping multi-well avalanche detectors (SWADs)," *Proc. SPIE*, vol. 10948, Mar. 2019, Art. no. 109481H, doi: 10.1117/12.2512470.

[17] R. J. Acciavatti and A. D. A. Maidment, "Non-stationary model of oblique X-ray incidence in amorphous selenium detectors: I. Point spread function," *Med. Phys.*, vol. 46, no. 2, pp. 494–504, 2019. doi: 10.1002/mp.13313.

[18] R. J. Acciavatti and A. D. A. Maidment, "Nonstationary model of oblique X-ray incidence in amorphous selenium detectors: II. Transfer functions," *Med. Phys.*, vol. 46, no. 2, pp. 505–516, 2019, doi: 10.1002/mp.13312.

[19] L. B. Schein, "Charge generation from band-gap states in amorphous selenium films," *Phys. Rev. B, Condens. Matter*, vol. 10, no. 8, pp. 3451–3457, 1974, doi: 10.1103/physrevb.10.3451.

[20] M. Zhu, G. Niu, and J. Tang, "Elemental Se: Fundamentals and Its optoelectronic applications," *J. Mater. Chem. C*, vol. 7, no. 8, pp. 2199–2206, 2019, doi: 10.1039/c8tc05873c.

[21] A. H. Goldan, J. A. Rowlands, O. Tousignant, and K. S. Karim, "Unipolar time-differential charge sensing in non-dispersive amorphous solids," *J. Appl. Phys.*, vol. 113, no. 22, 2013, Art. no. 224502, doi: 10.1063/1.4807292.

[22] M. Z. Kabir and N. Hijazi, "Temperature and field dependent effective hole mobility and impact ionization at extremely high fields in amorphous selenium," *Appl. Phys. Lett.*, vol. 104, no. 19, 2014, Art. no. 192103, doi: 10.1063/1.4876239.

[23] G. Hajdok, J. J. Battista, and I. A. Cunningham, "Fundamental X-ray interaction limits in diagnostic imaging detectors: Spatial resolution," *Med. Phys.*, vol. 35, no. 7Part1, pp. 3180–3193, 2008, doi: 10.1118/1.2924219.

[24] J. Stavro, A. H. Goldan, and W. Zhao, "Photon counting performance of amorphous selenium and its dependence on detector structure," *J. Med. Imag.*, vol. 5, no. 4, 2018, Art. no. 043502, doi: 10.1117/1.jmi.5.4.043502.

[25] J. Stavro, A. H. Goldan, and W. Zhao, "SWAD: Inherent photon counting performance of amorphous selenium multi-well avalanche detector," *Proc. SPIE*, vol. 9783, Mar. 2016, Art. no. 97833Q, doi: 10.1117/12.2217248.

[26] M. F. Stone, W. Zhao, B. V. Jacak, P. O'Connor, B. Yu, and P. Rehak, "The X-ray sensitivity of amorphous selenium for mammography," *Med. Phys.*, vol. 29, pp. 319–324, Mar. 2002.

[27] S. Kasap *et al.*, "Amorphous and polycrystalline photoconductors for direct conversion flat panel X-ray image sensors," *Sensors*, vol. 11, no. 5, pp. 5112–5157, 2011, doi: 10.3390/s110505112.

[28] S. Kasap, M. Z. Kabir, and J. A. Rowlands, "Recent advances in X-ray photoconductors for direct conversion X-ray image detectors," *Current Appl. Phys.*, vol. 6, no. 3, pp. 288–292, 2006, doi: 10.1016/j.cap.2005.11.001.

[29] S. O. Kasap and J. A. Rowlands, "Direct-conversion flat-panel X-ray image sensors for digital radiography," *Proc. IEEE*, vol. 90, no. 4, pp. 591–604, Apr. 2002, doi: 10.1109/jproc.2002.1002529.

[30] J. Rowlands and S. Kasap, "Amorphous semiconductors usher in digital X-ray imaging," *Phys. Today*, vol. 50, no. 11, pp. 24–30, 1997, doi: 10.1063/1.881994.

[31] G. Belev and S. O. Kasap, "Amorphous selenium as an X-ray photoconductor," *J. Non-Cryst. Solids*, vols. 345–346, pp. 484–488, Oct. 2004, doi: 10.1016/j.jnoncrysol.2004.08.070.

[32] S. O. Kasap, "X-ray sensitivity of photoconductors: Application to stabilized a-Se," *J. Phys. D, Appl. Phys.*, vol. 33, no. 21, pp. 2853–2865, Nov. 2000, doi: 10.1088/0022-3727/33/21/326.

[33] M. Z. Kabir and S. O. Kasap, "Charge collection and absorption-limited sensitivity of X-ray photoconductors: Applications to a-Se and HgI_2," *Appl. Phys. Lett.*, vol. 80, no. 9, pp. 1664–1666, 2002, doi: 10.1063/1.1454213.

[34] G. Juška and K. Arlauskas, "Features of hot carriers in amorphous selenium," *Phys. Status Solidi (A)*, vol. 77, no. 1, pp. 387–391, 1983, doi: 10.1002/pssa.2210770145.

[35] A. Reznik, S. D. Baranovskii, O. Rubel, K. Jandieri, and J. A. Rowlands, "Photoconductivity in amorphous selenium blocking structures," *Phys. Status Solidi (C)*, vol. 5, no. 3, pp. 790–795, 2008. doi: 10.1002/pssc.200777582.

[36] M. Z. Kabir, "Dark current mechanisms in amorphous selenium-based photoconductive detectors: An overview and re-examination," *J. Mater. Sci., Mater. Electron.*, vol. 26, no. 7, pp. 4659–4667, 2015, doi: 10.1007/s10854-015-2675-2.

[37] S. Abbaszadeh, N. Allec, K. Wang, and K. S. Karim, "Low dark-current lateral amorphous-selenium metal–semiconductor–metal photodetector," *IEEE Electron Device Lett.*, vol. 32, no. 9, pp. 1263–1265, Sep. 2011, doi: 10.1109/led.2011.2160327.

[38] J. B. Frey, G. Belev, O. Tousignant, H. Mani, L. Laperriere, and S. O. Kasap, "Dark current in multilayer stabilized amorphous selenium based photoconductive X-ray detectors," *J. Appl. Phys.*, vol. 112, no. 1, 2012, Art. no. 014502, doi: 10.1063/1.4730135.

[39] W. Zhao *et al.*, "Indirect flat-panel detector with avalanche gain: Fundamental feasibility investigation for SHARP-AMFPI (scintillator HARP active matrix flat panel imager)," *Med. Phys.*, vol. 32, no. 9, pp. 2954–2966, 2005, doi: 10.1118/1.2008428.

[40] S. Kasap, J. A. Rowlands, S. D. Baranovskii, and K. Tanioka, "Lucky drift impact ionization in amorphous semiconductors," *J. Appl. Phys.*, vol. 96, no. 4, pp. 2037–2048, 2004, doi: 10.1063/1.1763986.

[41] G. Juška and K. Arlauskas, "Impact ionization and mobilities of charge carriers at high electric fields in amorphous selenium," *Phys. Status Solidi (A)*, vol. 59, no. 1, pp. 389–393, 1980, doi: 10.1002/pssa.2210590151.

[42] A. LaBella, J. Stavro, S. Léveillé, W. Zhao, and A. H. Goldan, "Picosecond time resolution with avalanche amorphous selenium," *ACS Photon.*, vol. 6, no. 6, pp. 1338–1344, 2019, doi: 10.1021/acsphotonics.9b00012.

[43] M. Wronski, W. Zhao, K. Tanioka, G. Decrescenzo, and J. A. Rowlands, "Scintillator high-gain avalanche rushing photoconductor active-matrix flat panel imager: Zero-spatial frequency X-ray imaging properties of the solid-state SHARP sensor structure," *Med. Phys.*, vol. 39, no. 11, pp. 7102–7109, 2012, doi: 10.1118/1.4760989.

[44] A. Reznik *et al.*, "Avalanche multiplication phenomenon in amorphous semiconductors: Amorphous selenium versus hydrogenated amorphous silicon," *J. Appl. Phys.*, vol. 102, no. 5, 2007, Art. no. 053711. doi: 10.1063/1.2776223.

[45] K. Jandieri, O. Rubel, S. D. Baranovskii, A. Reznik, J. A. Rowlands, and S. O. Kasap, "Lucky-drift model for impact ionization in amorphous semiconductors," *J. Mater. Sci., Mater. Electron.*, vol. 20, no. S1, pp. 221–225, 2009, doi: 10.1007/s10854-007-9549-1.

[46] K. Tsuji, T. Ohshima, T. Hirai, N. Gotoh, K. Tanioka, and K. Shidara, "Ultra-high-sensitive image pickup tubes using avalanche multiplication in a-Se," *MRS Online Proc. Library Arch.*, vol. 219, p. 507, Feb. 2011, doi: 10.1557/proc-219-507.

[47] D. C. Hunt, K. Tanioka, and J. A. Rowlands, "X-ray imaging using avalanche multiplication in amorphous selenium: Investigation of intrinsic avalanche noise," *Med. Phys.*, vol. 34, no. 12, pp. 4654–4663, 2007, doi: 10.1118/1.2799494.

[48] K. Tanioka, J. Yamazaki, K. Shidara, K. Taketoshi, and T. Kawamura, "Advances in electronics and electron physics," in *Proc. 9th Symp. Held Imperial College, London, Adv. Electron. Electron Phys.* London, U.K.: Academic, Sep. 1988, p. 379.

[49] K. Tanioka *et al.*, "An avalanche-mode amorphous selenium photoconductive layer for use as a camera tube target," *IEEE Electron Device Lett.*, vol. 8, no. 9, pp. 392–394, Sep. 1987, doi: 10.1109/edl.1987.26671.

[50] K. Miyakawa *et al.*, "Ultrahigh-sensitivity HDTV new super-HARP camera," *Proc. SPIE*, vol. 5677, pp. 26–34, Mar. 2005, doi: 10.1117/12.585434.

[51] J. R. Scheuermann *et al.*, "Solid-state flat panel imager with avalanche amorphous selenium," *Proc. SPIE*, vol. 9783, Mar. 2016, Art. no. 978317, doi: 10.1117/12.2217002.

[52] S. M. Arnab and M. Z. Kabir, "Impact of Lubberts effect on amorphous selenium indirect conversion avalanche detector for medical X-ray imaging," *IEEE Trans. Radiat. Plasma Med. Sci.*, vol. 1, no. 3, pp. 221–228, May 2017, doi: 10.1109/trpms.2017.2692752.

[53] M. M. Wronski and J. A. Rowlands, "Direct-conversion flat-panel imager with avalanche gain: Feasibility investigation for HARP-AMFPI," *Med. Phys.*, vol. 35, no. 12, pp. 5207–5218, 2008, doi: 10.1118/1.3002314.

[54] D. C. Hunt, K. Tanioka, and J. A. Rowlands, "X-ray imaging using avalanche multiplication in amorphous selenium: Investigation of depth dependent avalanche noise," *Med. Phys.*, vol. 34, no. 3, pp. 976–986, 2007, doi: 10.1118/1.2437097.

[55] A. Sultana, A. Reznik, K. S. Karim, and J. A. Rowlands, "Design and feasibility of active matrix flat panel detector using avalanche amorphous selenium for protein crystallography," *Med. Phys.*, vol. 35, no. 10, pp. 4324–4332, 2008, doi: 10.1118/1.2975227.

[56] M. M. Wronski, W. Zhao, A. Reznik, K. Tanioka, G. Decrescenzo, and J. A. Rowlands, "A solid-state amorphous selenium avalanche technology for low photon flux imaging applications," *Med. Phys.*, vol. 37, no. 9, pp. 4982–4985, 2010, doi: 10.1118/1.3483096.

[57] A. Sultana, M. M. Wronski, K. S. Karim, and J. A. Rowlands, "Digital X-ray imaging using avalanche a-Se photoconductor," *IEEE Sensors J.*, vol. 10, no. 2, pp. 347–352, Feb. 2010, doi: 10.1109/jsen.2009.2034386.

[58] D. C. Hunt, S. S. Kirby, and J. A. Rowlands, "X-ray imaging with amorphous selenium: X-ray to charge conversion gain and avalanche multiplication gain," *Med. Phys.*, vol. 29, no. 11, pp. 2464–2471, 2002, doi: 10.1118/1.1513157.

[59] B. J. M. Lui, D. C. Hunt, A. Reznik, K. Tanioka, and J. A. Rowlands, "X-ray imaging with amorphous selenium: Pulse height measurements of avalanche gain fluctuations," *Med. Phys.*, vol. 33, no. 9, pp. 3183–3192, 2006, doi: 10.1118/1.2335491.

[60] N. Reznik, P. T. Komljenovic, S. Germann, and J. A. Rowlands, "Digital radiography using amorphous selenium: Photoconductively activated switch (PAS) readout system," *Med. Phys.*, vol. 35, no. 3, pp. 1039–1050, 2008, doi: 10.1118/1.2839279.

[61] A. Sultana, K. S. Karim, and J. A. Rowlands, "The effect of K- fluorescence reabsorption of selenium on the performance of an imaging detector for protein crystallography," *Phys. Status Solidi (C)*, vol. 6, no. S1, pp. S231–S235, 2009, doi: 10.1002/pssc.200881346.

[62] J. R. Scheuermann, A. H. Goldan, O. Tousignant, S. Léveillé, and W. Zhao, "Low dose digital X-ray imaging with avalanche amorphous selenium," *Proc. SPIE*, vol. 9412, Mar. 2015, Art. no. 94120E, doi: 10.1117/12.2081247.

[63] J. R. Scheuermann, A. H. Goldan, O. Tousignant, S. Léveillé, and W. Zhao, "Development of solid-state avalanche amorphous selenium for medical imaging," *Med. Phys.*, vol. 42, no. 3, pp. 1223–1226, 2015, doi: 10.1118/1.4907971.

[64] J. R. Scheuermann, A. Howansky, M. Hansroul, S. Léveillé, K. Tanioka, and W. Zhao, "Toward scintillator high-gain avalanche rushing photoconductor active matrix flat panel imager (SHARP-AMFPI): Initial fabrication and characterization," *Med. Phys.*, vol. 45, no. 2, pp. 794–802, 2017, doi: 10.1002/mp.12693.

[65] W. Shockley, "Currents to conductors induced by a moving point charge," *J. Appl. Phys.*, vol. 9, no. 10, pp. 635–636, 1938, doi: 10.1063/1.1710367.

[66] S. Ramo, "Currents induced by electron motion," *Proc. IRE*, vol. 27, no. 9, pp. 584–585, Sep. 1939, doi: 10.1109/jrproc.1939.228757.

[67] A. H. Goldan and K. S. Karim, "Unipolar charge sensing using Frisch grid technique for amorphous selenium radiation detectors," *Proc. SPIE*, vol. 7079, Sep. 2008, Art. no. 70790P, doi: 10.1117/12.796211.

[68] M. Z. Kabir and S. O. Kasap, "Charge collection and absorption-limited X-ray sensitivity of pixellated X-ray detectors," *J. Vac. Sci. Technol. A*, vol. 22, no. 3, p. 975, 2004, doi: 10.1116/1.1647588.

[69] H. H. Barrett, J. D. Eskin, and H. B. Barber, "Charge transport in arrays of semiconductor gamma-ray detectors," *Phys. Rev. Lett.*, vol. 75, no. 1, pp. 156–159, 1995, doi: 10.1103/physrevlett.75.156.

[70] K. S. Karim and A. Goldan, "Method and apparatus for a radiation detector," U.S. Patent 8 129 688 B2, Mar. 6, 2012.

[71] A. H. Goldan, O. Tousignant, K. S. Karim, and J. A. Rowlands, "Unipolar time-differential pulse response with a solid-state Charpak photoconductor," *Appl. Phys. Lett.*, vol. 101, no. 21, 2012, Art. no. 213503, doi: 10.1063/1.4766726.

[72] K. Wang *et al.*, "Amorphous-selenium-based three-terminal X-Ray detector with a gate," *IEEE Electron Device Lett.*, vol. 32, no. 6, pp. 782–784, Jun. 2011, doi: 10.1109/led.2011.2135836.

[73] R. E. Johanson, S. O. Kasap, J. Rowlands, and B. Polischuk, "Metallic electrical contacts to stabilized amorphous selenium for use in X-ray image detectors," *J. Non-Cryst. Solids*, vols. 227–230, pp. 1359–1362, May 1998, doi: 10.1016/s0022-3093(98)00310-x.

[74] K. Taguchi, C. Polster, O. Lee, and S. Kappler, "Spatio-energetic cross-talks in photon counting detectors: Detector model and correlated Poisson data generator," *Proc. SPIE*, vol. 9783, Mar. 2016, Art. no. 97831R, doi: 10.1117/12.2217133.

[75] J. Stavro, A. H. Goldan, and W. Zhao, "SWAD: The effect of pixel geometry on the spatial uniformity of avalanche gain," *Proc. SPIE*, vol. 10948, Mar. 2019, Art. no. 109483B, doi: 10.1117/12.2513365.

[76] D. L. Lee, H. Jang, A. Camlica, and K. S. Karim, "A novel radiation imaging detector with proportional charge gain," *Proc. SPIE*, vol. 10573, Mar. 2018, Art. no. 105735X, doi: 10.1117/12.2293429.

[77] A. Camlica, D. L. Lee, and K. S. Karim, "Increased temporal resolution of amorphous selenium detector using preferential charge sensing approach," *Proc. SPIE*, vol. 10573, Mar. 2018, Art. no. 105735W. doi: 10.1117/12.2293889.

[78] B. Zhao and W. Zhao, "Temporal performance of amorphous selenium mammography detectors," *Med. Phys.*, vol. 32, no. 1, pp. 128–136, 2004, doi: 10.1118/1.1827791.

[79] O. Tousignant, Y. Demers, L. Laperriere, H. Mani, P. Gauthier, and J. Leboeuf, "Spatial and temporal image characteristics of a real-time large area a-Se X-ray detector," *Proc. SPIE*, vol. 5745. pp. 207–215, Apr. 2005, doi: 10.1117/12.602183.

[80] M. Svobodová *et al.*, "Cutaneous leishmaniasis caused by Leishmania *infantum* transmitted by Phlebotomus *tobbi*," *Int. J. Parasitol.*, vol. 39, no. 2, pp. 251–256, 2009, doi: 10.1016/j.ijpara.2008.06.016.

[81] F. Nariyuki, S. Imai, H. Watano, T. Nabeta, and Y. Hosoi, "New development of large-area direct conversion detector for digital radiography using amorphous selenium with a C_{60}-doped polymer layer," vol. 7622, Mar. 2010, Art. no. 762240, doi: 10.1117/12.840788.

[82] S. Abbaszadeh, N. Allec, S. Ghanbarzadeh, U. Shafique, and K. S. Karim, "Investigation of hole-blocking contacts for high-conversion-gain amorphous selenium detectors for X-ray imaging," *IEEE Trans. Electron Devices*, vol. 59, no. 9, pp. 2403–2409, Sep. 2012, doi: 10.1109/ted.2012.2204998.

[83] K. Tanioka, "High-gain avalanche rushing amorphous photoconductor (HARP) detector," *Nucl. Instrum. Methods Phys. Res. A, Accel. Spectrom. Detect. Assoc. Equip.*, vol. 608, no. 1, pp. S15–S17, 2009, doi: 10.1016/j.nima.2009.05.066.

[84] T.-Y. Yu *et al.*, "Dark current suppression of amorphous selenium based photosensors by the ZnO hole blocking layer," *Current Appl. Phys.*, vol. 14, no. 5, pp. 659–664, 2014, doi: 10.1016/j.cap.2014.02.011.

[85] S. Abbaszadeh, C. C. Scott, O. Bubon, A. Reznik, and K. S. Karim, "Enhanced detection efficiency of direct conversion X-ray detector using polyimide as hole-blocking layer," *Sci. Rep.*, vol. 3, no. 1, p. 3360, 2013, doi: 10.1038/srep03360.

[86] C. C. Scott *et al.*, "Amorphous selenium direct detection CMOS digital X-ray imager with 25 micron pixel pitch," *Proc. SPIE*, vol. 9033, Mar. 2014, Art. no. 90331G, doi: 10.1117/12.2043770.

[87] K. Kikuchi *et al.*, "Hole-blocking mechanism in high-gain avalanche rushing amorphous photoconductor (HARP) film," *Phys. Status Solidi (C)*, vol. 8, no. 9, pp. 2800–2803, 2011, doi: 10.1002/pssc.201084055.

[88] S. Abbaszadeh, A. Tari, W. S. Wong, and K. S. Karim, "Enhanced dark current suppression of amorphous selenium detector with use of IGZO hole blocking layer," *IEEE Trans. Electron Devices*, vol. 61, no. 9, pp. 3355–3357, Sep. 2014, doi: 10.1109/ted.2014.2341249.

[89] C.-Y. Chang, F.-M. Pan, J.-S. Lin, T.-Y. Yu, Y.-M. Li, and C.-Y. Chen, "Lateral amorphous selenium metal-insulator-semiconductor-insulator-metal photodetectors using ultrathin dielectric blocking layers for dark current suppression," *J. Appl. Phys.*, vol. 120, no. 23, 2016, Art. no. 234501, doi: 10.1063/1.4972029.

[90] J. D. John *et al.*, "Modifying the electronic properties of Se/n-Si heterostructure using electrolysis," *Phys. Status Solidi (B)*, vol. 256, Feb. 2018, Art. no. 1800445, doi: 10.1002/pssb.201800445.

[91] S. O. Kasap and C. Juhasz, "Time-of-flight drift mobility measurements on chlorine-doped amorphous selenium films," *J. Phys. D, Appl. Phys.*, vol. 18, no. 4, pp. 703–720, 1985, doi: 10.1088/0022-3727/18/4/015.

[92] S. O. Kasap, K. V. Koughia, B. Fogal, G. Belev, and R. E. Johanson, "The influence of deposition conditions and alloying on the electronic properties of amorphous selenium," *Semiconductors*, vol. 37, no. 7, pp. 789–794, 2003, doi: 10.1134/1.1592851.

[93] S. O. Kasap and C. Juhasz, "Charge transport in selenium based amorphous xerographic photoreceptors," *Photograph. Sci. Eng. SPSE*, vol. 26, pp. 239–244, Nov. 1982. [Online]. Available: https://spiral.imperial.ac.uk/bitstream/10044/1/36323/2/Kasap-SO-1983-PhD-Thesis.pdf

[94] K. Koughia, Z. Shakoor, S. O. Kasap, and J. M. Marshall, "Density of localized electronic states in a-Se from electron time-of-flight photocurrent measurements," *J. Appl. Phys.*, vol. 97, no. 3, 2005, Art. no. 033706, doi: 10.1063/1.1835560.

[95] I. T. D. Dash, G. Belev, H. Mani, and S. Kasap, "Electronic and thermal properties of magnesium-doped a-Se films," *Phys. Status Solidi (C)*, vol. 6, no. S1, pp. S98–S101, 2009, doi: 10.1002/pssc.200881283.

[96] T. A. Chowdhury, C. Oner, and K. C. Mandal, "Synthesis and characterization of amorphous selenium alloys radiation detectors," in *Proc. IEEE Nucl. Sci. Symp. Med. Imag. Conf. (NSS/MIC)*, Oct. 2017, pp. 1–5, doi: 10.1109/nssmic.2017.8532698.

[97] I. Saito *et al.*, "A transparent ultraviolet triggered amorphous selenium p-n junction," *Appl. Phys. Lett.*, vol. 98, no. 15, 2011, Art. no. 152102, doi: 10.1063/1.3579262.

[98] M. Onishi *et al.*, "Characterization of a-Se p–i–n junction fabricated using bidirectional electrolysis in NaCl(aq)," *Phys. Status Solidi (A)*, vol. 212, no. 10, pp. 2322–2325, 2015, doi: 10.1002/pssa.201532372.

[99] H. Kroemer, "Heterostructure devices: A device physicist looks at interfaces," *Surf. Interfaces, Phys. Electron.*, vol. 132, pp. 543–576, Sep. 2002, doi: 10.1016/b978-0-444-86784-1.50043-2.

[100] K. Tanioka, "Ultra-high-sensitivity new super-HARP pickup tube," in *Proc. IEEE Workshop CCD Adv. Image Sensors*, Jun. 2001, pp. 216–219.

[101] W. Zhao, J. A. Rowlands, S. Germann, D. F. Waechter, and Z. Huang, "Digital radiology using self-scanned readout of amorphous selenium: Design considerations for mammography," *Proc. SPIE*, vol. 2432, pp. 250–259, May 1995, doi: 10.1117/12.208343.

[102] W. Zhao and J. A. Rowlands, "X-ray imaging using amorphous selenium: Feasibility of a flat panel self-scanned detector for digital radiology," *Med. Phys.*, vol. 22, no. 10, pp. 1595–1604, 1995, doi: 10.1118/1.597628.

[103] J. A. Rowlands, W. Zhao, I. M. Blevis, D. F. Waechter, and Z. Huang, "Flat-panel digital radiology with amorphous selenium and active-matrix readout," *RadioGraphics*, vol. 17, no. 3, pp. 753–760, 1997, doi: 10.1148/radiographics.17.3.9153709.

[104] M. J. Yaffe and J. A. Rowlands, "X-ray detectors for digital radiography," *Phys. Med. Biol.*, vol. 42, no. 1, pp. 1–39, Jan. 1997, doi: 10.1088/0031-9155/42/1/001.

[105] W. Zhao, I. Blevis, S. Germann, J. A. Rowlands, D. Waechter, and Z. Huang, "Digital radiology using active matrix readout of amorphous selenium: Construction and evaluation of a prototype real-time detector," *Med. Phys.*, vol. 24, no. 12, pp. 1834–1843, 1997, doi: 10.1118/1.598098.

[106] D. L. Y. Lee, L. K. Cheung, L. S. Jeromin, E. F. Palecki, and B. G. Rodricks, "New digital detector for projection radiography," *Proc. SPIE*, vol. 2432, pp. 88–96, May 1995, doi: 10.1117/12.208342.

[107] D. L. Y. Lee, L. K. Cheung, E. F. Palecki, and L. S. Jeromin, "Discussion on resolution and dynamic range of Se-TFT direct digital radiographic detector," *Proc. SPIE*, vol. 2708, pp. 511–522, Apr. 1996, doi: 10.1117/12.237813.

[108] N. M. Sheth *et al.*, "Imaging performance of CMOS and a-Si:H flat-panel detectors for C-arm fluoroscopy and cone-beam CT," *Proc. SPIE*, vol. 10573, Mar. 2018, Art. no. 105730M, doi: 10.1117/12.2293780.

[109] A. Parsafar, C. C. Scott, A. El-Falou, P. M. Levine, and K. S. Karim, "Direct-conversion CMOS X-ray imager with 5.6 μm $\times$ 6.25 μm pixels," *IEEE Electron Device Lett.*, vol. 36, no. 5, pp. 481–483, May 2015, doi: 10.1109/led.2015.2410304.

[110] C. C. Scott, A. Parsafar, A. El-Falou, P. M. Levine, and K. S. Karim, "High dose efficiency, ultra-high resolution amorphous selenium/CMOS hybrid digital X-ray imager," in *IEDM Tech. Dig.*, Dec. 2015, pp. 30.6.1–30.6.4, doi: 10.1109/iedm.2015.7409803.

[111] A. Camlica, A. El-Falou, R. Mohammadi, P. M. Levine, and K. S. Karim, "CMOS-integrated single-photon-counting X-ray detector using an amorphous-selenium photoconductor with 11×11-μm^2 pixels," in *IEDM Tech. Dig.*, Dec. 2018, pp. 32.5.1–32.5.4, doi: 10.1109/iedm.2018.8614645.

[112] K. S. Karim, M. H. Izadi, F. Taghibakhsh, and G. Sanaie, "Intelligent pixel architectures for digital medical imaging applications," *ECS Trans.*, vol. 8, no. 1, pp. 289–293, 2007, doi: 10.1149/1.2767322.

[113] K. Wang *et al.*, "Integration of an amorphous silicon passive pixel sensor array with a lateral amorphous selenium detector for large area indirect conversion X-ray imaging applications," *Proc. SPIE*, vol. 7961, Mar. 2011, Art. no. 79610V, doi: 10.1117/12.877592.

[114] T.-T. Kuo, C.-M. Wu, H.-H. Lu, I. Chan, K. Wang, and K.-C. Leou, "Flexible X-ray imaging detector based on direct conversion in amorphous selenium," *J. Vac. Sci. Technol. A*, vol. 32, no. 4, 2014, Art. no. 041507, doi: 10.1116/1.4882835.

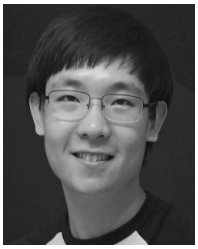

Heyuan Huang is currently pursuing the B.S. degree with the University of Illinois at Urbana–Champaign, through the dual-degree program of physics and nuclear engineering, with the concentration on radiological, medical, and instrumentation applications. In 2017, he joined Shiva Abbaszadeh's Research Group, where he has participated in researches concerning PET scanners and X-ray imagers. In summer 2018, he was a Physics Intern with GE Healthcare, where he helped to improve the manufacturing process of X-ray panels.

Shiva Abbaszadeh received the Ph.D. degree from the Electrical and Computer Engineering Department (ECE), University of Waterloo, ON, Canada. She was an Assistant Professor with the University of Illinois at Urbana–Champaign. She is currently an Assistant Professor with ECE, University of California at Santa Cruz, Santa Cruz. Her research interests include radiation detection and instrumentation for molecular imaging, computational problem solving, and quantitative characterization of biological processes.